Spin-Density-Wave Antiferromagnetism in the Chromium System I: Magnetic Phase Diagrams, Impurity States, Magnetic Excitations and Structure in the SDW Phase

Eric Fawcett

Physics Department, University of Toronto,

Toronto M5S 1A7, Canada

Abstract

The chromium system, comprising pure Cr and alloys with most transition metals and some non-transition metals, is the archetypical spin-density-wave (SDW) system. This paper supplements, with a brief summary and extension to include recent work, two previous comprehensive reviews on Cr (Fawcett, 1988) and Cr alloys (Fawcett et al., 1994). The magnetic phase diagrams are reviewed. Impurity states in CrFe and CrSi, when suitably doped with V or Mn, produce dramatic effects in the electrical resistivity, including a low-temperature resistance minimum due to impurity-resonance scattering. Curie–Weiss paramagnetism appears just above the Néel temperature in dilute CrV alloys. Recent work on inelastic neutron scattering in pure Cr is reviewed: the apparent absence of dispersion of the spin-wave modes at the wave vectors of the incommensurate SDW where the Bragg satellite peaks occur; the energy-dependent anisotropy of the excitations in the longitudinal-SDW phase; the commensurate magnetic scattering at the centre of the magnetic zone, which at higher energy and temperature dominates the inelastic scattering at the satellites; the Fincher–Burke excitations seen at low-energy in the transverse-SDW phase; and the silent satellites seen in single-Q Cr at off-axis incommensurate points as temperature increases towards the Néel transition. X-ray scattering with synchrotron radiation has illuminated the relation between the SDW in Cr and the incommensurate charge-density wave that accompanies it.

1 Introduction

Chromium is the archetypical itinerant antiferromagnet, whose incommensurate spin-density wave (SDW) has a wave vector Q determined by the nesting properties of its Fermi surface. At the same time, the persistence of antiferromagnetism in Cr alloys over a wide range of compositions, when considered in the light of its absence in Mo and W, whose Fermi surfaces are very similar to that of pure Cr,

indicates that the $3d$ character of this metal is of fundamental importance to its being magnetic.

The beauty and the mystery of Cr and its alloys do not derive from their being antiferromagnets, of which there are many, but from the fact that they constitute a SDW antiferromagnetic system. The richness of the magnetic phenomena observed in the Cr system is a consequence of the SDW's being a truly many-body effect.

The present paper, and the companion papers (Fawcett et al., 1997; Fawcett, 1997, which are referred to as Papers II and III, respectively) summarize the reviews of SDW antiferromagnetism in Cr, by Fawcett (1988: referred to as RMP I), and in Cr alloys, by Fawcett et al. (1994: referred to as RMP II), with discussion especially of those areas where significant new advances have since been made. Some of the most active workers in the field presented papers at the 1996 Yamada Conference in a symposium having the same title as the present paper, which will accordingly summarize only very briefly their findings and refer the reader to the 1996 Yamada Conference Proceedings for a more complete account and further references (Alberts and Smit, 1997; Fishman et al., 1997; Hayden et al., 1997; Tsunoda, 1997; see also Fishman and Liu, 1993, 1994, 1996).

Section 2 reviews magnetic phase diagrams in the composition-temperature x–T plane. Impurity states, discussed in Sect. 3, offer new possibilities for understanding interesting properties of some Cr alloys. Recent experiments, which exploit the enhanced sensitivity of the SQUID magnetometer in studies of the temperature and field dependence of their magnetic susceptibility, show that Curie–Weiss paramagnetism occurs in dilute CrV alloys just above the Néel temperature; and that spin-glass behaviour occurs in CrMn and ternary alloys of Cr containing Mn (see Paper II, Fawcett et al., 1997). In both cases, presumably, a moment exists on the impurity atom, but there is no theoretical understanding of these phenomena.

The final Sect. 4 deals with inelastic neutron scattering in pure Cr. The magnetic excitation spectra of Cr and its SDW alloys are so rich in unusual phenomena that they continue to elude our understanding, despite considerable experimental efforts by several groups. We shall discuss here briefly, but with generous illustrations of the original data, so that the reader will have a fairly comprehensive picture of the behaviour: the energy-dependent anisotropy of the excitations in the longitudinal-SDW phase; the so-called "Fincher–Burke" excitations seen at low energy, $E \leq 8$ meV, in the transverse-SDW phase; the so-called "commensurate magnetic scattering" (CMS) at the centre of the magnetic zone, which grows with energy and temperature until it dominates the spin-wave scattering at the incommensurate satellite points in both the longitudinal- and transverse-SDW phases; and the so-called "silent satellites", which are low-energy critical fluctuations that grow rapidly close to the Néel temperature at the off-axis incommensurate points in single-Q Cr, thus leading to the return to cubic symmetry in the paramagnetic

phase with the disappearance of the SDW at the weakly first-order Néel transition.

Critical scattering in the paramagnetic phase in pure Cr and dilute CrV alloys (Noakes et al., 1990), and the so-called "SDW paramagnons" that occur close to the quantum critical point in the paramagnetic alloy $Cr_{95}V_5$ (Fawcett et al., 1988; Hayden et al., 1997) are discussed in relation to new high-temperature thermal expansion results in Paper II (Fawcett et al., 1997).

The remarkable similarity of the magnetic phase diagrams in the composition-temperature and composition-pressure planes is discussed in Paper III (Fawcett, 1997) in relation to the strong volume-dependence of the magnetism in the Cr system. This is reflected in dramatic effects in the temperature dependence of the physical properties of Cr and its SDW alloys, which persist to temperatures much greater than the Néel transition, as discussed in Paper II. A striking example of this parallelism between the effects of composition change and pressure in ternary CrFeV alloys is described in Paper III.

2 Magnetic phase diagrams

Chromium alloys exhibit four magnetic phases: longitudinal SDW (AF_2), transverse SDW (AF_1), commensurate SDW (AF_0), and paramagnetic magnetic (P). The general features of the phase diagram may be explained in terms of the canonical model for SDW antiferromagnetism in the Cr alloy system, which comprises nesting electron and hole octahedra, with a reservoir of electrons corresponding to the rest of the Fermi surface. This model was first worked out in detail by Shibatani et al. (1969), following the idea of the SDW proposed originally by Overhauser (1960, 1962). The model was further developed by Kotani (a new name for Shibatani), in a series of papers referenced in RMP II, to include the effects of the charge-density wave and of scattering of electrons by impurities. These two effects have featured large in recent theoretical work by Fishman et al. (1997, and references therein).

Figure 1 illustrates the systematics of the phase diagram for most alloys of Cr with transition metals. The metals from Group IB (Au), Group IV (Ti) and Group V (V, and also Nb and Ta not shown here) depress the Néel temperature T_N with increasing concentration, and eventually destroy the SDW at a concentration of a few atomic percent. Group VII (Mn, Re) and Group VIII (all the other elements shown in Fig. 1), apart from the ferromagnetic metals Fe, Co and Ni (and also Pd), raise T_N, with the appearance at a concentration of a fraction of a percent (see Table IV in RMP II) of the commensurate SDW phase AF_0. With changing composition x of the solute metal, T_N rises rapidly beyond the triple point, while the transition temperature T_{IC} between the AF_0 and AF_1 phases drops rapidly to
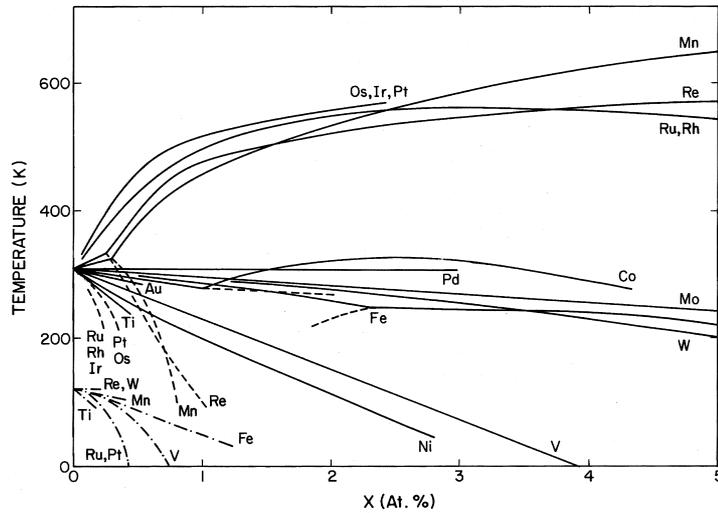
Figure 1. Schematic magnetic phase diagram for alloys $Cr_{1-x}A_x$ of chromium with transition metals A. ——— T_N, Néel temperature; — — — — T_{IC}, transition temperature from the incommensurate SDW AF_1 phase to the commensurate SDW AF_0 phase; — · — · — T_{SF}, spin-flip temperature from the transverse-SDW phase AF_1 to the longitudinal-SDW phase AF_2.

zero. Thus, when $x > 1$ to 2 at.%, the SDW remains commensurate all the way from T_N to zero temperature.

This behaviour is well understood qualitatively in terms of the canonical model and a rigid band picture for which transition metals in Groups IV and V lower the Fermi level, thereby decreasing the nesting between the electron and hole octahedra, and conversely for Group VII and VIII metals. The pioneer experimental work in this field was done by Allan Mackintosh and his co-workers (Møller and Mackintosh, 1965, Møller et al., 1965; Koehler et al., 1966) and the Japanese group (Hamaguchi and Kunitomi, 1964) using neutron diffraction.

The typical behaviour for larger concentrations of a Group VIII transition metal dissolved in Cr is illustrated in Fig. 2. Interest in the nature of the phase boundary between the SDW phase and the superconducting phase, and the possible coexistence of the two states goes back to the study of CrRe by Muheim and Müller (1964). Subsequent work on both CrRe and CrRu, both of which systems are superconducting for compositions close to the SDW phase, have however been inconclusive (see Sect. VI.E in RMP II).

The depression of T_N by the Group VI metals Mo and W, which are isoelectronic with Cr and have a very similar Fermi surface, with however increasing width of the
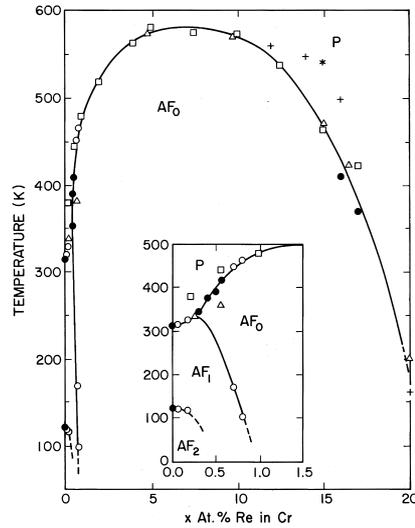
Figure 2. Magnetic phase diagram for the $Cr_{1-x}Re_x$ alloy system (see Fig. 13 in RMP II for sources of the experimental data).

d-bands from $3d$ to $4d$ to $5d$, is presumably due to their reduction of the exchange and correlation interactions responsible for the occurrence of the SDW rather than to change in the Fermi level (see also Fig. 3b and comments on it below).

Inspection of Fig. 1 shows that the systems CrFe, CrNi and CrPd do not follow these simple rules. Considerable efforts have been made to understand, in particular, the unique phase diagram of CrFe, in which the AF_1 phase occurs at higher temperature than the AF_0 phase, i.e., the dash-line showing $T_{IC}(x)$ goes to the left towards lower values of x in Fig. 1 (Galkin et al., 1997b). A similar effect occurs in CrSi also (Endoh et al., 1982), but very soon the $T_{IC}(x)$ line turns back to the normal behaviour giving a re-entrant AF_0 phase very close to the triple point (see Fig. 17 in RMP II). The model of Nakanishi and Kasuya (1977) was most successful in explaining this effect in CrFe (see Fig. 57b in RMP II), but it relies upon an arbitrary magnetoelastic term in the free energy, and a fundamental explanation is lacking. This term however reproduces the large magnetostriction that is seen at the strongly first order Néel transition to the AF_0 phase in CrFe (Butylenko, 1989; see Fig. 1 in Fawcett and Galkin, 1992). CrSi also exhibits a large first order magnetostriction at the Néel transition to the AF_0 phase (Suzuki, 1977), but it is difficult to understand the commonality between the two alloy systems.

For several alloys of Cr with non-transition metals the phase diagram is rather similar to that for Cr with Group VIII transition metals, as shown in Fig. 3. These
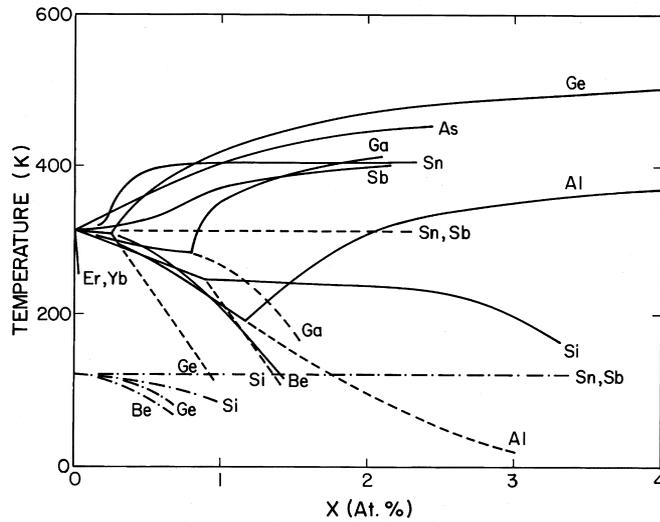
Figure 3. Schematic magnetic phase diagram for alloys $Cr_{1-x}A_x$ of chromium with non-transition metals A. ———— T_N, Néel temperature; — — — — T_{IC}, non-transition temperature from the incommensurate SDW AF_1 phase to the commensurate SDW AF_0 phase; — · — · — T_{SF}, spin-flip temperature from the transverse-SDW phase AF_1 to the longitudinal-SDW phase AF_2.

are all substitutional alloys, but there is no reason whatsoever to believe that the effect of a non-transition metal like Ge on the band structure of Cr is similar to that of Ru, for example. One looks in vain for an alternative to the canonical model to explain the behaviour of alloys of Cr with non-transition metals.

We select for more detailed discussion the CrAl alloy system, whose magnetic phase diagram is shown in Fig. 4. Alternative interpretations of the experimental data are shown, but the dash-line is now thought to be incorrect and serves only to illustrate the difficulties encountered sometimes in mapping out the phase diagram, in this case probably due to errors in determining the alloy compositions.

The behaviour of the $Cr_{1-x}Al_x$ alloy system for x up to 30 at.% Al shown in Fig. 4a is quite remarkable. The value of T_N approaches 800 K, a value higher than that for any other system. There is some evidence that for the higher concentrations, $x > 15$ at.% Al, CrAl is a narrow-gap semiconductor, which would mean that the moments are localized rather than existing in a SDW (Fawcett et al., 1994).

Figure 4b shows how the introduction of 5 at.% Mo so dilutes the Cr host, thereby reducing the exchange and correlation interactions, that the SDW disappears in the ternary alloys for $2 \leq x \leq 5$ at.% Al (Smit and Alberts, 1987).

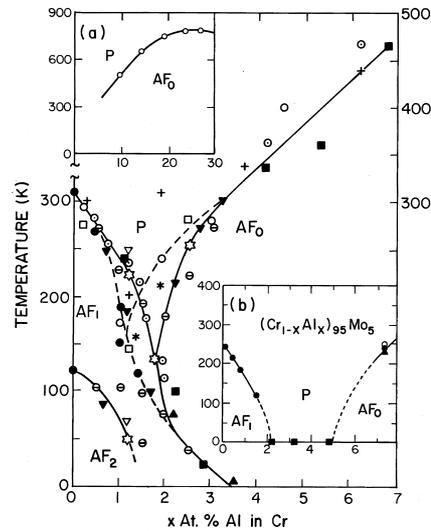Finally we note in Figs. 1 and 3 that the spin-flip transition temperature de-

Figure 4. Magnetic phase diagram for the $Cr_{1-x}Al_x$ alloy system. Insert (a) shows the phase diagram for higher concentrations of Al, and insert (b) shows the phase diagram for the ternary alloy system $(Cr_{1-x}Al_x)_{95}Mo_5$ (see Fig. 16 in RMP II for sources of the experimental data).

creases rapidly to zero with increasing solute concentration for all alloy systems (except CrSn and CrSb, but for these the experimental data are suspect). A satisfactory explanation of the spin-flip transition in pure Cr is still wanted (RMP I).

3 Impurity states

Allan Mackintosh and his co-workers (Møller et al., 1965; Trego and Mackintosh, 1968) performed the first systematic study of the temperature dependence of the electrical resistivity $\rho(T)$ and the thermopower $S(T)$ of SDW alloys of Cr with V, Mn, Mo, W, and Re (and also neutron diffraction in the same alloys, Koehler et al., 1966). As well as finding qualitative agreement between the variation of the Néel temperature with electron concentration and an early version of the canonical model for the Cr system, they observed effects associated with the electron-hole condensation responsible for the formation of the SDW in Cr (Overhauser, 1962). Their results for CrV alloys are shown in Fig. 5. The increase of $\rho(T)$ with decreasing T below the Néel transition seen in Fig. 5a is largely due to the formation of an energy gap on the nesting parts of the Fermi surface, where the electron–hole
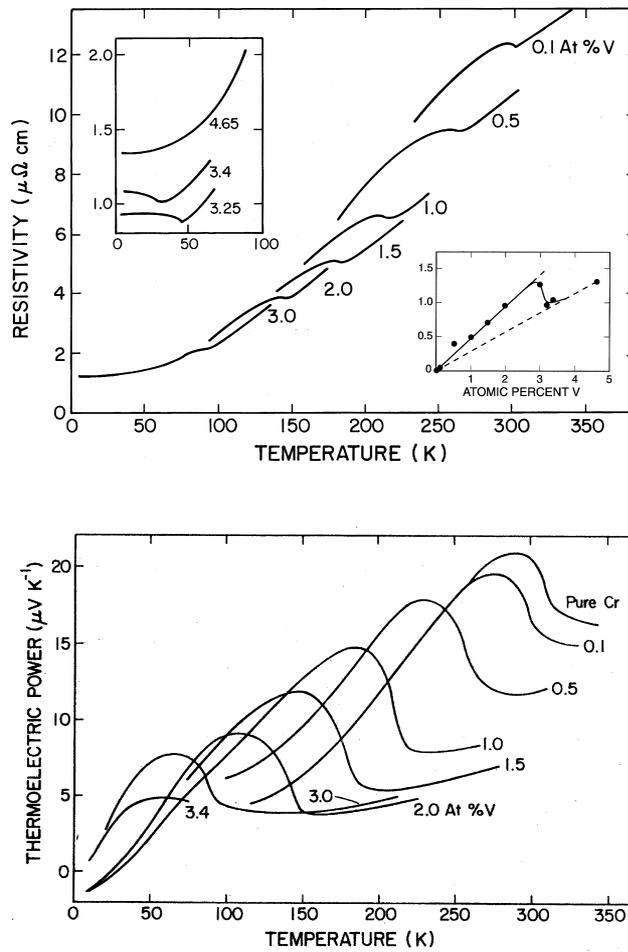
Figure 5. (a) Temperature dependence of the resistivity of $Cr_{1-x}V_x$ alloys, for compositions ranging from $x = 0.1$ to 4.65 at.% V in Cr. The inset shows the residual resistivity at temperature 4.2 K as a function of V concentration. (b) Temperature dependence of the thermoelectric power of the same CrV alloys (after Trego and Mackintosh, 1968)

pairs do not contribute to electrical conduction. The effect is seen in pure Cr and it is anisotropic in a single-Q sample (see Fig. 47 in RMP I) because the nesting occurs along and thus defines the wave vector Q of the SDW. The condensation of the electrons and holes also changes the scattering of single-particle carriers, which is largely due to phonons in the temperature region of interest. The hump in $\rho(T)$ below T_N results from a combination of these two factors, and in some alloys is much larger than in pure Cr (see Table VI in RMP II).

The anomaly in $S(T)$ shown in Fig. 5b is similar in form to that of $\rho(T)$, but is more pronounced. The explanation (Trego and Mackintosh, 1968) is that the thermopower is proportional to the derivative of the resistivity with respect to energy of electrons/holes at the Fermi surface, $S \sim -d\ln\rho/dE$. Thus, while the decrease in the scattering almost cancels the increase in resistivity due to the condensation with decreasing temperature, giving rise to only a small hump in $\rho(T)$ below T_N, as seen in Fig. 7a, the energy dependence of the two effects that determine the thermopower results in two terms that have the same sign and together give the large hump in $S(T)$. In dilute $Cr_{1-x}Mn_x$ alloys ($x \leq 3.4$ at.% Mn), Trego and Mackintosh (1968) found that $S(T)$ exhibits a low-temperature hump, which increases in amplitude relative to the value in the paramagnetic phase as x increases, and showed that the form of the temperature dependence provides clear evidence that it is due to phonon drag.

Although there is a vast literature on impurity states in normal metals, ferromagnetic metals and semiconductors, this aspect of the theory and practice for SDW alloys in the Cr system has been neglected. The use of local probes, principally the Mössbauer effect, diffuse neutron scattering, perturbed angular correlation and nuclear magnetic resonance, to explore a limited number of Cr alloys has provided desultory information about a few impurity atoms dissolved in Cr and in the SDW phase (RMP II).

The theory of local impurity states within the antiferromagnetic energy gap opened up by the electron-hole condensation (Volkov and Tugushev, 1984; Tugushev, 1992) offered new possibilities for understanding the behaviour of SDW Cr alloys with non-magnetic as well as magnetic metals. Until now these possibilities have been little explored, though the potential for discovering new phenomena is no doubt as rich as it was for impurity states in the forbidden energy band of semiconductors. Those predicted by Tugushev's theory include: resonant scattering by the impurity state, which gives rise to an additional term in the residual resistivity at zero temperature, and a negative temperature-dependent contribution $\rho_{res}(T) \sim -T^2$, when the Fermi level is close to one of the pair of impurity levels predicted by the theory; and a negative magneto-resistance in the case when the pair of impurity levels are spin-polarized.

The best evidence to support the theory of local impurity states is illustrated
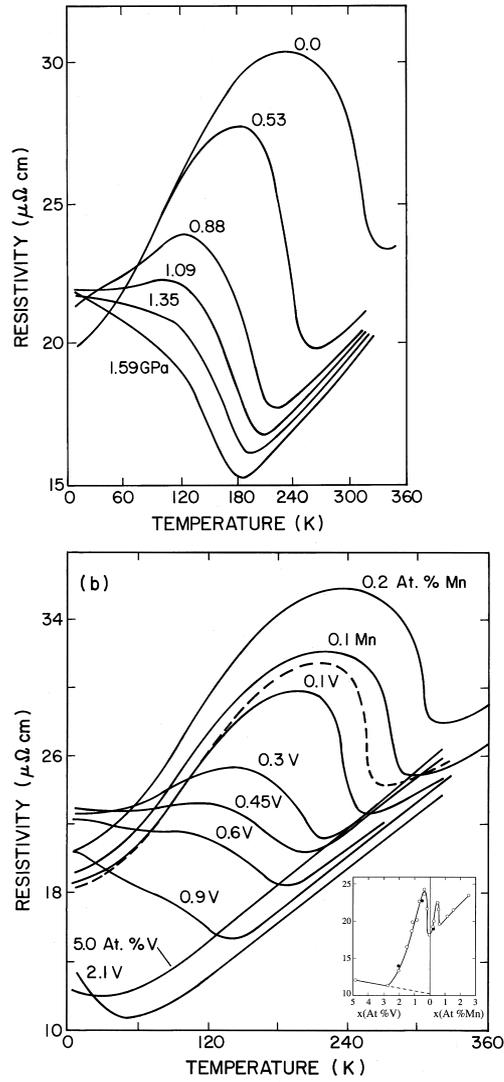
Figure 6. (a) Pressure dependence of the resistivity of Cr+2.7 at.% Fe+0.27% Mn (from Galkin, 1989). (b) Temperature dependence of the resistivity of ternary alloys (Cr+2.7 at.% Fe)$_{1-x}$(V,Mn)$_x$, with the concentrations x of V or Mn shown on the curves, the curve for undoped Cr+2.7 at.% Fe being dashed (after Galkin and Fawcett, 1993). The inset shows the residual resistivity at temperature 4.2 K as a function of alloy composition (from Galkin, 1989).

in the inset to Fig. 6b. The two peaks in the concentration dependence of the residual resistivity are believed to correspond to the energy levels of the pair of impurity states of the Fe atom, with doping by (V,Mn) being employed only to tune the Fermi level. Fawcett and Galkin (1991) have analyzed this data and also measurements by Galkin (1987) on $(Cr+1.3 \text{ at.\% Si})_{1-x}(V,Mn)_x$, and find that the splitting between the pair of energy levels is about the same, 24 to 28 meV, of the order of 10% of the energy gap in a commensurate SDW Cr alloy (see Fig. 70 in RMP II).

It seems likely that the resistance minimum seen in several Cr alloy systems (see Table VI in RMP II) is due to the predicted negative term in the resistivity, $\rho_{\text{res}}(T) \sim -T^2$. Katano and Mori (1979) attribute the minimum in $\rho(T)$ seen in CrFe alloys (see Fig. 29 in RMP II) to the Kondo effect associated with the moment on the Fe impurity that gives rise to the Curie–Weiss temperature dependence of the susceptibility in the SDW phase, but none of the other Cr alloys that exhibit a low-temperature resistivity minimum have a moment according to this criterion. When the term $\rho_{\text{res}}(T)$ is combined with other temperature-dependent terms in the resistivity, the behaviour of $\rho(T)$ becomes rather complex, and the curves in Figs. 6a and 6b, for example, still have not been analyzed. Paper III (Fawcett, 1997) describes work by Galkin et al. (1997c) that shows convincingly that the minimum in CrFeV alloys in the SDW phase is due to impurity-resonance scattering, but when the system is brought into the paramagnetic phase by doping or the application of pressure it becomes a shallower Kondo minimum.

V and Mn have been generally regarded, ever since the construction of the canonical model, which together with a rigid-band model explained very nicely the dependence of the wave vector Q and the Néel temperature T_N on the composition of dilute Cr(V,Mn) alloys, as doing nothing more than tune the Fermi level by adding (Mn) or removing (V) electrons from the host Cr. It turns out in fact that V strongly affects many other physical properties, including (Fawcett, 1992) inelastic neutron scattering, nuclear magnetic relaxation time, the nature of the Néel transition, electrical resistivity in the paramagnetic phase, and the magneto-elastic properties. We shall consider here only the appearance with V doping of a component of the susceptibility $\chi(T)$ in the paramagnetic phase having a temperature dependence that obeys a Curie–Weiss law (Hill et al., 1994). CrMn alloys, on the other hand, have been found to exhibit remarkable spin-glass properties at low temperatures (Galkin et al., 1995, 1996a, 1996b, 1997a). The absence of a Curie–Weiss law for $\chi(T)$ in the SDW phase had been generally assumed to mean that the Mn atom carries no moment in SDW $Cr_{1-x}Mn_x$ alloys for $x \leq 10$ at.% Mn (Maki and Adachi, 1979).

Figure 7 shows the data for $\chi(T)$ in two dilute CrV alloys in comparison with that for pure Cr. The Curie–Weiss paramagnetism evident here is not seen in CrV
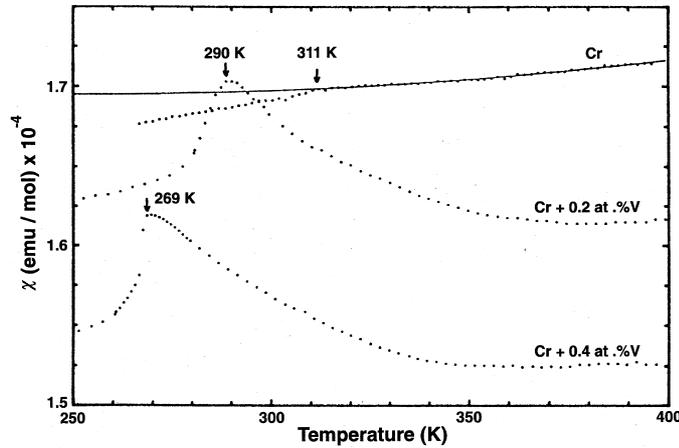
Figure 7. Temperature dependence of the magnetic susceptibility $\chi(T)$ of pure Cr and two dilute CrV alloys. The line through the data points above the Néel temperature, $T_N = 311$ K, for Cr is a quadratic fit to $\chi(T)$ (from Hill et al., 1994).

alloys containing more than $x \geq 0.67$ at.% V, and is suppressed in a measuring field, $H = 6$ kOe (de Oliviera et al., 1996b).

No theory is available to explain any of these unexpected experimental results. They have been made possible, like the discovery of spin-glass behaviour in CrMn alloys, by the advent of highly sensitive methods of measuring the magnetic susceptibility with low measuring fields, either by use of a SQUID magnetometer (Hill et al., 1994) or of an AC susceptometer (de Oliviera et al., 1996a). It is quite likely that other alloys of Cr with non-magnetic metals will be found, when re-examined more carefully by use of these methods, to exhibit Curie–Weiss paramagnetism. It is well-known that Fe and Co, as well as Mn, carry a moment in the paramagnetic phase of their alloys with Cr (see Table V in RMP II). In the case of CrRe, CrRh and CrSi there may already be some evidence for the existence of local moments above T_N, in that, for concentrations high enough to be well into the AF$_0$ phase, there are some compositions for which $\rho(T)$ decreases with increasing temperature above T_N (see the references in Table V in RMP II).

4   Neutron scattering in the SDW phase

The spectrum of magnetic excitations in Cr is rich in modes that are still largely not explained at even the most rudimentary level. The so-called "spin-wave" modes are
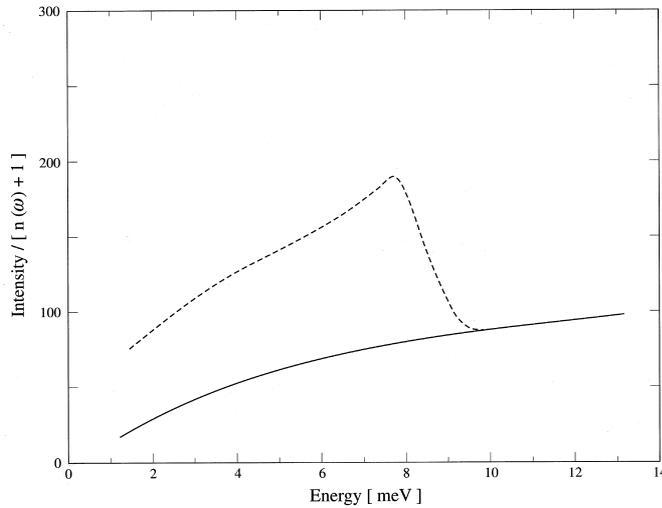
Figure 8. Anisotropy of spin fluctuations in the longitudinal-SDW phase of Cr: peak intensity for single-Q Cr in the longitudinal-SDW AF$_2$ phase at temperatures from 10 to 100 K, normalized by the thermal factor $[n(\omega) + 1]^{-1}$: ———— at $(2\pi/a)$ $(1-\delta, 0, 0)$ from longitudinal q-scans (see Fig. 11b); — — — — at $(2\pi/a)(\delta, 1, 0)$ from transverse q-scans (after Lorenzo et al., 1994).

conceived as lying on a a dispersion cone emanating, in the case of a single-Q sample with wave vector Q along x, from the incommensurate points at $\pm Q_x = (2\pi/a)$ $(1 \pm \delta)$, δ being the incommensurability parameter, as illustrated in the inset (b) of Fig. 11. Theory predicts that their velocity will be of the same order of magnitude as the Fermi velocity of the electrons and holes that condense to form the triplet pairs constituting the SDW. Experiments on CrMn alloys having a commensurate SDW seem to support this idea (see Table I in RMP I). There is, however, no clear evidence for such dispersion in pure Cr, though the inelastic scattering peaks at the satellites do increase in width roughly linearly with increasing energy (see Fig. 5 in Fukuda et al., 1996).

The spin-wave modes in the longitudinal-SDW phase have an unusual energy-dependent anisotropy, as illustrated in Fig. 8. For energy below, $E \leq 8$ meV, the excitations are predominantly longitudinal, while for higher energy they are isotropic. The intensity scaled by the thermal factor, $[n(\omega) + 1]^{-1}$, $n(\omega = E/\hbar)$ being the Bose-Einstein distribution function, is independent of temperature in the longitudinal-SDW phase. The analysis can be taken further (Lorenzo et al., 1994) by assuming a linear dispersion relation for the spin-wave mode, with the result that the longitudinal and transverse components of the dynamic susceptibility, $\chi_L(E)$
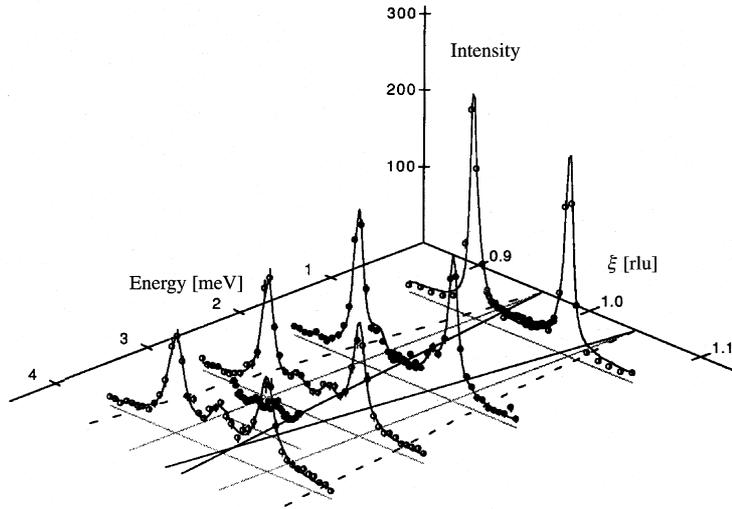
Figure 9. Fincher–Burke modes: longitudinal *q*-scans at constant energy, $E =$ 0.75, 2 ,3, 3.5 and 4 meV, along $(\xi, 0, 0)$ (the solid arrow in Fig. 3b) for single-*Q* Cr in the transverse-SDW phase at temperature 230 K. The peaks of intensity I (arbitrary units) are projected into the *E*–ξ plane: ——— the SDW satellites at $(2\pi/a)(1 \pm \delta, 0, 0)$; ——— the modes seen between the SDW satellites; — — — — the modes *not* seen outside the SDW satellites (after Sternlieb et al., 1993).

and $\chi_T(E)$, respectively, vary as the reciprocal of *E*. This is the same as for $\chi_T(E)$ for spin waves in an antiferromagnet having localized moments, but in this case, $\chi_L(E) = 0$. Burke et al. (1983) pointed out that longitudinal excitations, in the form of propagating crystal-field modes, are found in many rare-earth metals and compounds, but that no other case is known in 3*d* metals and alloys.

In the transverse-SDW phase, modes of excitation appear between the unresolved spin-wave peaks at $\pm Q_x = (2\pi/a)(1 \pm \delta)$ in a single-*Q* sample. These Fincher–Burke modes were first thought to have dispersion relations that are symmetric about $\pm Q_x$, having a velocity the same as that of the $(\xi, 0, 0)$ longitudinal phonons (Burke et al., 1983). As illustrated in Fig. 9, however, there is no evidence for inelastic scattering peaks for $\xi < -Q_x$ or $\xi > +Q_x$. Thus their identification as magneto-vibrational modes is incorrect.

Pynn et al. (1992) also found that the intensity of the 4 meV peak at $(2\pi/a)$ $(1, 0, 0)$, where the two modes intersect (see Fig. 9), increases in intensity with increasing temperature much faster than one would expect for a mode involving phonons. They used polarized neutrons and found that the scattering at this 4

meV peak involves spin fluctuations parallel to the polarization direction of the transverse SDW. The susceptibility $\chi_{FB}(E)$ of these modes, like the spin-wave modes in the longitudinal-SDW phase, varies as the reciprocal of the energy E (Lorenzo et al., 1994). These clues may help us to understand the origin of the Fincher–Burke modes.

Fishman and Liu (1996) have analyzed the low-energy magnetic excitations of the incommensurate-SDW phase of Cr. They find two Goldstone modes evolving from the incommensurate points, transverse spin waves, and longitudinal phasons. But their velocity is of the same order of magnitude as the Fermi velocity, about two orders larger than the Fincher–Burke modes. Thus the origin of the low-energy excitations remains a mystery.

At higher energies, in both the longitudinal- and transverse-SDW phase, a broad scattering peak develops at the commensurate point, $(2\pi/a)(1,0,0)$. Fukuda et al. (1996) find that this commensurate magnetic scattering (CMS), as illustrated in Fig. 10, increases with both energy E and temperature T, until it overwhelms the incommensurate scattering due to the spin-wave modes by $E = 40$ meV at $T = 54$ K in the longitudinal-SDW phase (Fig. 10a), or by $T = 235$ K at $E = 15$ meV in the transverse-SDW phase (Fig. 10h). In the longitudinal-SDW AF_2 phase the integrated intensity of the CMS increases roughly linearly with energy, whereas the intensity of the spin-wave mode peaks at $E \approx 20$ meV (see Fig. 6a in Fukuda et al., 1996).

This magnetic scattering at the magnetic-zone centre was first studied by the BNL group (Fincher et al., 1981; Grier et al., 1985), who described it as "commensurate-diffuse scattering" (CDS). It appeared to increase in intensity very rapidly as temperature approached the Néel transition, but this feature of the behaviour has been shown to be an instrumental artifact associated with the existence of the silent satellites (Sternlieb et al., 1995). The characteristic energy, $E \approx 4$ meV, of the CDS should also rather be considered as a feature of the Fincher–Burke modes (see Fig. 9). Thus we prefer to use the new acronym CMS, rather than CDS, to describe the broad high-energy scattering peak at the magnetic-zone centre. The latter may still however be the appropriate term for the scattering at the commensurate point seen in the paramagnetic phase at high temperatures, up to and beyond $2T_N$ (see Figs. 13 and 14 in Grier et al., 1985). Whether or not CMS and CDS are manifestations in different temperature regimes of the same modes of excitation will not be known until we have an explanation of commensurate scattering in Cr, whose origin is still a complete mystery.

Sternlieb et al. (1995) realized the significance for pure Cr of the existence in the paramagnetic alloy, Cr+5 at.%V, of spin fluctuations at the incommensurate points corresponding to the nesting vector Q' of the Fermi surface (Fawcett et al., 1988). One might expect to find a peak in the wave-vector dependent susceptibility $\chi(q)$ at
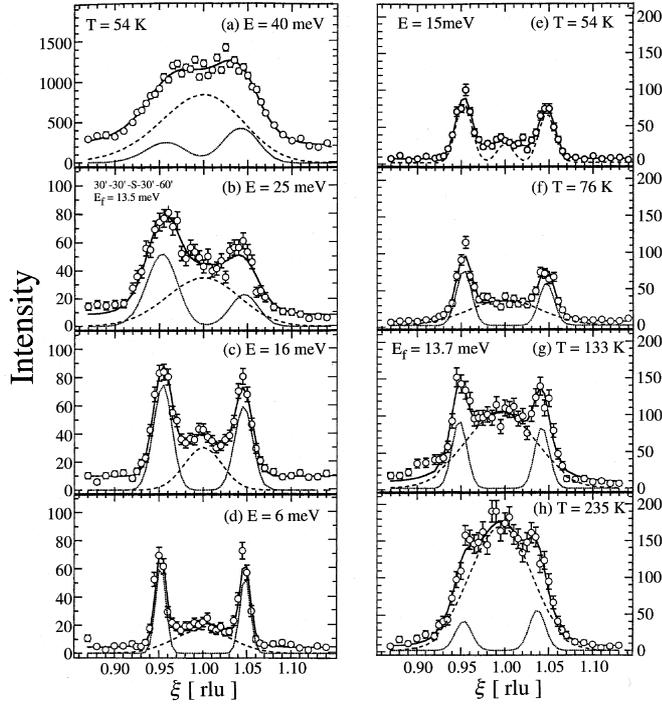
Figure 10. Commensurate Magnetic Scattering (CMS): longitudinal constant-E scans (the solid arrow in Fig. 3b) for single-Q Cr at various energies E at temperature, $T = 54$ K (panels a, b, c and d), and for various T at $E = 15$ meV (panels e, f, g and h). The dash and light lines are the CMS and incommensurate SDW components, respectively, which together with a constant background give the resultant solid line fit to the data (from Fukuda et al., 1996).

Q', which becomes a singularity corresponding to the onset of long-range magnetic order, i.e., a SDW with $Q \approx Q'$, when the V content is reduced to less than about 4 at.%V (RMP II). Thus, in a single-Q sample of Cr with $Q = (2\pi/a)(1 \pm \delta, 0, 0)$, the other two pairs of off-axis satellites at $(2\pi/a)(1, \pm\delta, 0)$ and $(2\pi/a)(1, 0, \pm\delta)$ might be expected to give rise to peaks in $\chi(q)$, with corresponding modes of excitation giving inelastic scattering at these points.

Figure 11 illustrates the experimental evidence for these silent satellites. As temperature increases towards the Néel temperature T_N, their intensity increases rapidly from very low values, until at T_N a discontinuous jump (corresponding to the first-order nature of the Néel transition in Cr) results in equal scattering at all six satellites corresponding to the cubic symmetry of the paramagnetic phase. Thus
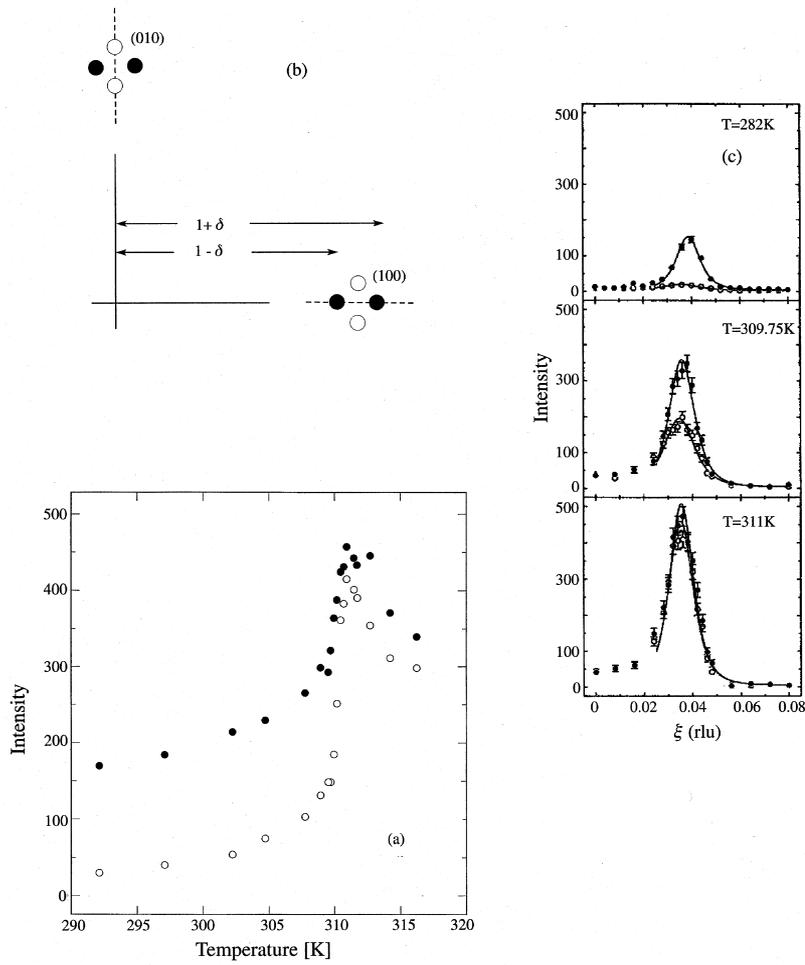
Figure 11. Silent satellites: (a) temperature dependence of the peak intensity for longitudinal scans at constant energy, $E = 0.5$ meV, for single-Q Cr: ● corresponds to the q-scan ——— in inset (b); ○ corresponds to the q-scan − − − − in inset (b). Inset (c) shows the data for the complete q-scan close to the Néel temperature, $T_N = 310.3$ K, and at a temperature 28 K below T_N (after Sternlieb et al., 1995).

the Néel transition is driven by critical fluctuations at all six satellites, not just at the two at the wave vectors $\pm Q_x$ of the SDW. This picture of the relation between the spin-wave excitations and the critical fluctuations is unique to Cr, but its theoretical analysis should enlarge our general understanding of phase transitions.

The Chalk River group first recognized that the apparent commensurate-diffuse scattering in the paramagnetic phase, at least close to the Néel temperature and at low energies, is in fact an instrumental artifact (Noakes et al., 1990). Thus a constant-energy scan through the satellites at $Q = (2\pi/a)(1 \pm \delta, 0, 0)$ will pick up the off-axis satellites (the silent satellites in the case of a single-Q sample) if the momentum resolution transverse to the $(1, 0, 0)$ axis is poor as usually is the case. This does not of course preclude the existence of genuine commensurate modes of excitation at high energies in the ordered phase (Fig. 10) or at high temperatures in the paramagnetic phase (Grier et al., 1985).

Synchrotron radiation is a powerful tool for studying the charge-density wave that is present in Cr (Tsunoda et al., 1974; Pynn et al., 1976) and Cr alloys (RMP II). When x-rays of energy ≈ 10 keV are used, the technique is limited to the study of the surface of the sample, since they penetrate only to a depth of about 1 μm. This may account for the fact that in the measurements of Hill et al. (1995) the results corresponded to there being a single Q-direction, normal to the (100) surface of the sample, since residual strain from the mechanical polishing may have been sufficient to cause this effect. It may also have something to do with the failure thus far to see the CDW in any Cr alloys.

Conceptually there are two mechanisms a density wave in the charge distribution. First, the lattice may be periodically distorted, with each ion retaining its equilibrium charge: a strain wave. Second, there may be a periodic excess and deficit of charge on the sites of an undistorted lattice. In the CDW literature, these two effects are collectively referred to as a charge-density wave. Both produce x-ray diffraction peaks at $2Q$ and $4Q$. The dominant contribution to the x-ray scattering intensity arises from the core electrons of the ion, and thus corresponds to the strain wave. Mori and Tsunoda (1993) attempted to separate the two contributions, and claim that they found a small conduction-electron density wave in addition to the dominant contribution from the strain wave.

Hill et al. (1995) found that in Cr the intensities of elastic scattering due the the fundamental SDW and the second and fourth harmonic CDW had temperature dependence throughout both the AF_1 and AF_2 phases corresponding to mean-field theory.

Acknowledgements

References

Alberts HL and Smit P, 1997: Proceedings of the 1996 Yamada Conf., Physica B (In press)

Burke SK, Stirling WG, Ziebeck KRA and Booth JG, 1983: Phys. Rev. Lett. **51**, 494

Butylenko AK, 1989: Fiz. Met. Metalloved. **68**, 873 [Phys. Met. Metallogr. (USSR) **68**, 37 (1989)]

de Oliviera AJA, Ortiz WA, de Camargo PC and Galkin VYu, 1996a: J. Magn. Magn. Mater. **152**, 86

de Oliviera AJA, de Lima OF, de Camargo PC, Ortiz WA and Fawcett E, 1996b: J. Phys. Condens. Matter **8**, L403

Endoh Y, Mizuki J and Ishikawa Y, 1982: J. Phys. Soc. Jpn. **51**, 263

Endoh Y, 1996: (private communication)

Fawcett E, 1988: Rev. Mod. Phys. **60**, 209

Fawcett E, Werner SA, Goldman A and Shirane G, 1988: Phys. Rev. Lett. **61**, 558.

Fawcett E, and Galkin VYu, 1991: J. Phys. Condens. Matter **3**, 7167

Fawcett E, 1992: J. Phys. Condens. Matter **4**, 923

Fawcett E and Galkin VYu, 1992: J. Magn. Magn. Mater. **109**, L139

Fawcett E, Alberts HL, Galkin VYu, Noakes DR and Yakhmi JV, 1994: Rev. Mod. Phys. **66**, 25

Fawcett E, de Camargo PC, Galkin VYu and Noakes DR, 1997: Proceedings of the 1996 Yamada Conf., Physica B (In press)

Fawcett E, 1997: Proceedings of the 1996 Kumamoto Conf., Physica B (In press)

Fert A, Grunberg P, Barthelemy A, Petroff F and Zinn W, 1995: J. Magn. Magn. Mater. **140-144**, 1

Fincher JCR, Shirane G and Werner SA, 1979: Phys. Rev. Lett. **43**, 1441

Fishman RS and Liu SH, 1993: J. Phys. Condens. Matter **5**, 3959

Fishman RS and Liu SH, 1994: Phys. Rev. B **50**, 4240

Fishman RS and Liu SH, 1996: Phys. Rev. Lett. **76**, 2398

Fishman RS, Liu SH and Viswanath VS, 1997: Proceeding of the 1996 Yamada Conf., Physica B (In press)

Fukuda T, Endoh Y, Yamada K, Takeda M, Itoh S, Arai M and Otomo T, 1996: J. Phys. Soc. Jpn. **65**, 1418

Galkin VYu, 1987: Fiz. Met. Metalloved. **624**, 1199 [Phys. Met. Metallogr. (USSR) **64**, 150 (1987)]

Galkin VYu, 1989: J. Magn. Magn. Mater. **79**, 327

Galkin VYu and Fawcett E, 1993: J. Magn. Magn. Mater. **119**, 321

Galkin VYu, de Camargo PC, Ali N, Schaf J and Fawcett E, 1995: J. Phys. Condens. Matter **7**, L649

Galkin VYu, de Camargo PC, Ali N, Schaf J and Fawcett E, 1996a: J. Magn. Magn. Mater. **159**, 1

Galkin VYu, de Camargo PC, Ali N and Fawcett E, 1996b: J. Phys. Condens. Matter (in press)

Galkin VYu, de Camargo PC, Ali N and Fawcett E, 1997a: Proceedings of the 1996 Yamada Conf., Physica B

Galkin et al., 1997b: Proceedings of the 1996 MMM Conf., J. Appl. Phys. (In press)

Galkin et al., 1997c: Proceedings of the 1996 MMM Conf., J. Appl. Phys. (In press)

Grier BH, Shirane G and Werner SA, 1985: Phys. Rev. B **31**, 2882

Hayden SM, Doubble R, Aeppli G, Fawcett E, Perring TG, Lowden J, and Mitchell PW, 1997: Proceedings of the 1996 Yamada Conf., Physica B (In press)

Hamaguchi Y, and Kunitomi N, 1964: J. Phys. Soc. Jpn. **19**, 1849

Heinrich B, and Bland JAC (ed.), 1994: *Ultrathin Magnetic Structures* (Springer-Verlag, Berlin), Chapter 2

Hill P, Ali N, de Oliveira AJA, Ortiz WA, de Camargo PC and Fawcett E, 1994: J. Phys. Condens. Matter **6**, 1761

Hill JP, Helgesen G and Gibbs D, 1995: Phys. Rev. B **51**, L77

Katano S and Mori N, 1979: J. Phys. Soc. Jpn. **46**, 691

Koehler WC, Moon RM, Trego AL and Mackintosh AR, 1966: Phys. Rev. **151**, 405

Lorenzo JE, Sternlieb BJ, Shirane G and Werner SA, 1994: Phys. Rev. Lett. **72**, 1762

Maki S and Adachi K, 1979: J. Phys. Soc. Jpn. **46**, 1131

Møller HB and Mackintosh AR, 1965: Phys. Rev. Lett. **15**, 623

Møller HB, Trego AL and Mackintosh AR, 1965: Solid State Commun. **3**, 137

Mori M and Tsunoda Y, 1993: J. Phys. Condens. Matter **5**, L77

Muheim S and Müller, 1964: Phys. Kondens. Mater. **2**, 377

Nakanishi K, and Kasuya T, 1977: J. Phys. Soc. Jpn. **42**, 833

Noakes DR, Holden TM, Fawcett E and de Camargo PC, 1990a: Phys. Rev. Lett. **65**, 369

Overhauser AW, 1960: Phys. Rev. Lett. **4**, 226

Overhauser AW, 1962: Phys. Rev. **128**, 1437

Pynn R, Press W, Shapiro SM and Werner SA 1976: Phys. Rev. B **13**, 295

Pynn R, Stirling WG and Savering A, 1992: Physica B **180-181**, 203

Shibatani A, Motizuki K and Nagamiya T, 1969: Phys. Rev. **177**, 984

Smit P and Alberts HL, 1987: J. Phys. Chem. Solids **48**, 887

Sternlieb BJ, Shirane G, Werner A and Fawcett E, 1993: Phys. Rev. B **48**, 10217

Suzuki T, 1977: J. Phys. Soc. Jpn. **43**, 869

Trego AL and Mackintosh AR, 1968: Phys. Rev. **166**, 495

Tsunoda Y, Mori M, Kunitomi N, Teraoka Y and Kanamori J, 1974: Solid State Commun. **14**, 287

Tsunoda Y, 1997: Proceedings of the 1996 Yamada Conf., Physica B (In press)

Tugushev VV, 1992: in *Electronic Phase Transitions*, eds. by W. Hanke and Yu.V. Kipaev (Elsevier, New York/Amsterdam) p. 237

Volkov BA and Tugushev VV, 1984: Fiz. Tverd. Tela (Leningrad) **26**, 2428 [Sov. Phys. Solid State **26**, 1471 (1984)]